laval Research Laboratory

ıshington, DC 20375-5320

NRL/MR/6440–92-7170

Shock-Free Acceleration of Laser Driven Targets

MARK H. EMERY AND JOHN H. GARDNER

Center for Computational Physics Branch
Computational Physics and Fluids Dynamics Division

December 10, 1992

REPORT DOCUMENTATION PAGE

Form Approved
OMB No. 0704-0188

1. AGENCY USE ONLY (*Leave Blank*)	2. REPORT DATE	3. REPORT TYPE AND DATES COVERED
	December 10, 1992	Interim

4. TITLE AND SUBTITLE

Shock-Free Acceleration of Laser Driven Targets

5. FUNDING NUMBERS

PE 61103
PR 6068
TA 55
WU 2926A2

6. AUTHOR(S)

Mark H. Emery and John H. Gardner

7. PERFORMING ORGANIZATION NAME(S) and ADDRESS(ES)

Naval Research Laboratory
Washington, DC 20375-5320

8. PERFORMING ORGANIZATION REPORT NUMBER

NRL/MR/6440--92-7170

9. SPONSORING/MONITORING AGENCY NAME(S) AND ADDRESS(ES)

Department of Energy
Washington, DC 20375-5320

10. SPONSORING/MONITORING AGENCY REPORT NUMBER

11. SUPPLEMENTARY NOTES

12a. DISTRIBUTION/AVAILABILITY STATEMENT

Approved for public release, distribution is unlimited

12b. DISTRIBUTION CODE

13. ABSTRACT (*Maximum 200 words*)

The ability of recently developed laser smoothing techniques to produce uniform ablation pressures is strongly contingent on the degree of thermal smoothing. Thermal smoothing is not effective at reducing residual laser nonuniformities during the start up phase of a shaped, reactor-like laser pulse. The impact of the first shock can be diminished by adiabatically compressing the target with a temporally long, slowly rising laser pulse. This Memorandum Report discusses an elastic-plastic laser-matter-interaction model and shows that a shock-free, induced spatial incoherence-smoothed laser pulse can accelerate a target to nearly the conditions required for uniform implosion.

14. SUBJECT TERMS

Laser smoothing
laser-target interaction
elastic-plastic
adiabatic compression

15. NUMBER OF PAGES

16

16. PRICE CODE

17. SECURITY CLASSIFICATION OF REPORT	18. SECURITY CLASSIFICATION OF THIS PAGE	19. SECURITY CLASSIFICATION OF ABSTRACT	20. LIMITATION OF ABSTRACT
UNCLASSIFIED	UNCLASSIFIED	UNCLASSIFIED	UL

SHOCK-FREE ACCELERATION OF LASER DRIVEN TARGETS

A high degree of ablation pressure uniformity is a necessary criterion for the success of laser driven inertial confinement fusion. Asymmetries in the ablation pressure must remain less than a few percent throughout the implosion process if high gain is to be achieved.[1] This places a severe requirement of the uniformity of the laser illumination. The ability of the recently developed random phase plate (RPP)[2], smoothing by spectral dispersion (SSD)[3], and induced spatial incoherence (ISI)[4] laser smoothing techniques to produce a nearly uniform ablation pressure is strongly contingent on the degree of thermal smoothing in the ablating plasma.[4,5] The SSD and ISI techniques benefit from temporal smoothing as a result of the broadband nature of the laser light but residual nonuniformities persist with all three methods. Nearly all shaped reactor-like laser pulses are composed of four distinct phases : (1) an initial rapid rise to a low - to - moderate intensity, (2) a long temporal, low intensity "foot", (3) a moderately rapid (power law-like) rise to high intensity, and (4) the main drive portion of the pulse. See Figure 1. The first two regimes are usually referred to as the start-up phase, and the ratio of the final drive power to the foot power is termed the dynamic range. The details of the actual pulse shape (initial rise time, duration of the "foot", dynamic range, and final drive intensity) are dictated by the target design (material composition, layered/nonlayered, target thickness) and the desired final velocity of the target; but, in general, the pulse is designed so that the initial shock keeps the target on a low adiabat and breaks out through the rear of the target as the laser intensity reaches the beginning of the drive portion of the pulse.

Manuscript approved October 20, 1992.

Thermal smoothing is not effective at reducing any inherent laser beam nonuniformities during the "foot" portion of the pulse and the shock structure generated during the start-up phase will mirror any residual laser nonuniformities.[5] The resulting small initial mass perturbations can linearly grow a order of magnitude or more, depending on the target thickness, as a result of the Richtmyer-Meshkov instability[6] before the target begins the rapid acceleration phase.[5] It is the mass variations near the beginning of the drive portion of the laser pulse which will provide the seeds for Rayleigh-Taylor[7] (RT) growth during the acceleration phase. For a target to implode uniformly, the mass variations at this point must be $\ll 1\%$. Recent numerical results[5] indicate that cold, low density foam layers, multiple wavelength lasers and initial x-ray flashes can significantly reduce the mass perturbation level stemming from the initial imprint of an ISI-smoothed laser beam. There is also expermental evidence that an initial x-ray flash can eliminate plasma jetting generated by the initial imprint of an ISI-smoothed laser.[8] However, the numerical results indicate that the perturbation level at the beginning of the drive portion of the pulse (several percent) is still too large to enable the target to implode uniformly.[5] Since it is the first shock which is the culprit here, it may be possible to compress the target adiabatically - without any shocks except for the final drive portion of the pulse - and circumvent the problem. This would entail a very long, slowly rising laser pulse. A pulse of this shape would generate kilobar-like pressures in the target and thus compressive stress, shear stress, elastic response and plastic flow become important considerations. We have modified our numerical model to account for these phenomena and report on those results in this Memorandum Report.

Our two-dimensional, Cartesian, fully compressible hydrodynamics code with a sliding Eulerian grid with variable grid spacing and real equation of state has been modified to incorporate elastic, elastic-plastic, and hydrodynamic flow in a manner similar to the model developed by Wilkins.[9] The media is assumed to be isotropic and the stress terms in the conservation equations for momentum and energy are composed of a stress associated with a hydrostatic pressure and a stress associated with the resistance of the material to shear distortion. Hooke's law provides the linear correspondence between stress and strain for an elastic material through the Lame' constants which are material dependent. Plastic flow begins where the elastic distortion energy exceeds the von Mises yield condition.[10] Plastic flow is described by maintaining the stress deviators at the elastic limit so that the material flows plastically under a constant stress without work hardening. When enough work has been done to melt the material, the yield stress is set to zero and the hydrodynamic description follows automatically. The particulars of the model will be detailed in a forthcoming report.[11]

As a test of the model we simulate the response of a target impacted with a 1 nsec FWHM Gaussian 1/4 μm laser pulse with a peak intensity of 10^{10} W/cm^2. The target is composed of 35 μm of polystyrene ($\rho^o_{CH} = 1.04 gm/cm^3$) with a 45 μm thick layer of low density foam-like material ($\rho^o_{foam} = 0.08 gm/cm^3$) on the front surface (laser-side). This artificial foam-like material has material properties similar to a mixture of polystyrene and frozen DT. As the absorption characteristics of low intensity lasers is not well understood and is further complicated by the problems of material transparency and shine-through[12],

we assume that the targets are opaque to the laser light and the laser light is absorbed through inverse Bremsstrahlung absorption with 10% of the laser light that reaches critical deposited in three cells that surround the critical surface (in this case, the target surface). Figure 2 is an x-t diagram illustrating the elastic compression and tension waves propagating through the two materials. A 2-D perspective plot of the density of each material is plotted separately for clarity and the density is normalized to 1.0 in each case. When the laser "pings" the foam layer, an elastic compression wave is sent through the foam. When this wave reaches the plastic-foam interface, a portion is transmitted through the plastic and a portion is reflected back through the foam. As these compression waves reach the front and rear free surfaces, they are reflected as elastic tension waves and the cycle continues. Note that once the compression/tension wave has propagated through the material, the material relaxes back to its original density, there is little dissipation of the wave amplitude and little mass diffusion as evidenced by the steep gradients at the front surface of the target and at the material interface after 42 nsec, or 5 transits of the elastic waves. The maximum amplitude of the stress wave as in propagates through the media is approximately 5 kbar. See Figure 3. The yield strength of the foamlike material is 4.7 kbar and 40.8 kilobar for the plastic. The computational results yield an elastic wave velocity in the foam (plastic) of 5.42 x 10^5 cm/s (2.20 x 10^5 cm/s) as compared to the theoretical/experimental values of 5.39 x 10^5 cm/s (2.19 x 10^5 cm/s) [13] At the interface between two dissimilar materials, the amplitude of the transmitted stress wave (σ_t) should equal the sum of the amplitudes of the incident (σ_i) and reflected (σ_r) stress waves. For

stresses measured at the interface, the computational results give $\sigma_1 + \sigma_r = 5.45$ kbar and $\sigma_t = 5.5$ kbar. The computational results are in excellent agreement with theory.

For the adiabatic, slowly rising, high intensity laser pulse case, we chose target thicknesses and maximum laser intensities similar to those envisioned for the NIKE Laser System.[14] For the first case, the ISI-smoothed laser pulse has the canonical power-law profile with a 1/2 nsec rise to 10^{12} W/cm^2, a $t^{-5/4}$ rise to 3 x 10^{14} W/cm^2 at 6 nsec, followed by a 3 nsec drive at this intensity. See Figure 1. The target is 60 μm of CH, and the laser wavelength is 1/4 μm with a coherence time of 1 psec. The target mass variation at the beginning of the drive portion of the pulse (6 nsec) is 3.6%. This is comparable to the mass variation (3.8%) attained with the pure hydrodynamic version of the code under the same pulse shape conditions. This is to be expected as the first shock stemming from this laser pulse is O(1 Mbar) and the elasticity/plasticity of the material does not play a role. The target would soon fracture as a result of the RT instability with an initial mass perturbation of this magnitude. The total energy density of the laser pulse (9 nsec) is 970 kJ/cm^2 and the target velocity at 9 nsec is 2.5 x 10^7 cm/s.

For the shock-free pulse, the laser intensity starts at 10^7 W/cm^2 and increases very slowly reaching 3 x 10^{14} W/cm^2 at 28 nsec. See Figure 4a. Shown in Figure 4b is an x - t - ρ plot illustrating the target response. A small compression wave begins propagating through the target at $\approx$ 20 nsec; the total stress has reached an amplitude of $\approx$ 20 kbar at this time. The peak compressed density is 8.2 gm/cm^3 which is 12% larger than for the 6 nsec pulse case. Figure 5 illustrates the target isodensity contours at 28 nsec -

the beginning of the drive portion of the pulse. The amplitude of the maximum density variation is only 0.5%. This is close to the requirement ($O(0.1\%)$) for uniform implosion. Note that a portion of this growth, an e-folding or so, is due to RT growth as the target begins to rapidly accelerate at $\approx$ 27 nsec. For this case, the total energy density of the laser pulse (31 nsec) is 1200 kJ/cm^2 and the target velocity at 31 nsec is 2 x 10^7 cm/s.

In summary, we have shown that it is possible to minimize the impact of the residual nonuniformities inherent in a nonperfect laser beam during the start-up phase. This is done by eliminating the first shock in the laser pulse by designing a temporally long, slowly rising, truly adiabatic laser pulse. In order to model this phenomena, we developed an elastic, elastic-plastic, hydrodynamic code. A small price is paid in laser energy and hydrodynamic efficiency, but the net result is that the perturbation level is reduced by nearly an order of magnitude below the level attained with the canonical power-law pulse or with other target designs.[5]

Acknowledgements

This work was supported by the US DoE and ONR.

REFERENCES

1. S. E. Bodner. J. Fusion Energy **1**, 221(1981).

2. Y. Kato, K. Mima, N. Miyanaga, S. Arinaga, Y. Kitagawa, M. Nakatsuka, and C Yamanaka, Phys. Rev. Lett. **53**, 1057(1984).

3. S. Skupsky, R. W. Short, T. Kessler, R. S. Craxton, S. Letzring, and J. M. Soures, J Appl. Phys. **66**, 3456 (1989).

4. R. H. Lehmberg and S. P. Obenschain, Opt. Commun. **46**, 27(1983); R. H. Lehmberg, A. J. Schmitt, and S. E. Bodner, J. App. Phys. **62**, 2680 (1987).

5. M. H. Emery, J. H. Gardner, R. H. Lehmberg, and S. P. Obenschain, Phys. Fluids B **3**, 2640 (1992).

6. R. D. Richtmyer, Commun. Pure Appl. Math. **13**, 297 (1960); Ye. Ye. Meshkov, NASA Technical Translation NASA TT F-13, 074 (1970).

7. Lord Rayleigh, *Theory of Sound*, 2nd. ed. (Dover, New York, 1945, Vol 2). G. I Taylor, Proc. R. Soc. London Ser. **A 201**, 192 (1950).

8. M. Desselberger, T. Afshar-rad, F. Khattak, S. Viana, and O. Willi, Phys. Rev. Lett. **68**, 1539 (1992).

9. Mark L. Wilkins, Meth. Comp. Physics **3**, 211 (1964).

10. R. von Mises, *Z. Angew. Math. u. Mech.* **8** [Eng. trans. UCRL Trans. 872(L)] (1928).

11. M. H. Emery, in preparation.

12. J. Delettrez, D. K. Bradley, P. A. Jaanimagi, and C. P. Verdon, Phys. Rev. A. **41**, 5583 (1990).

13. *LASL Shock Hugoniot Data* , edited by Stanley P. Marsh, (Univ. Cal. Press, Los Angeles, 1980).

14. J. H. Gardner, J. P. Dahlburg, M. H. Emery, and S. E. Bodner, Bull. Am. Phys. Soc. **35**, 1969 (1990).

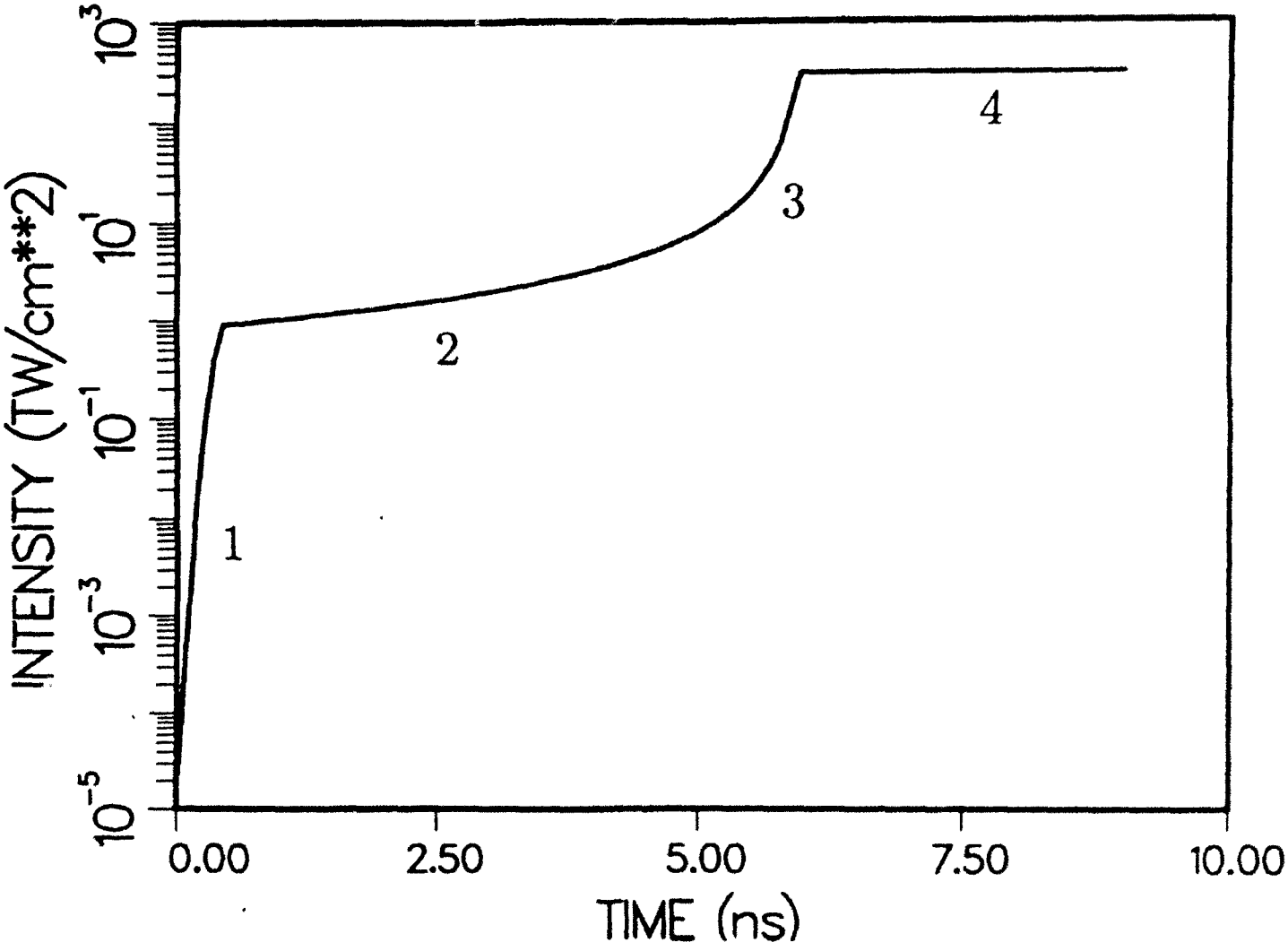

Figure 1. Plot of the intensity versus time of a typical power law laser pulse. The sections labeled 1 and 2 are the startup portion of the pulse, the drive portion of the pulse is labeled 4. This pulse shape is the canonical power law pulse for the NIKE Laser System.

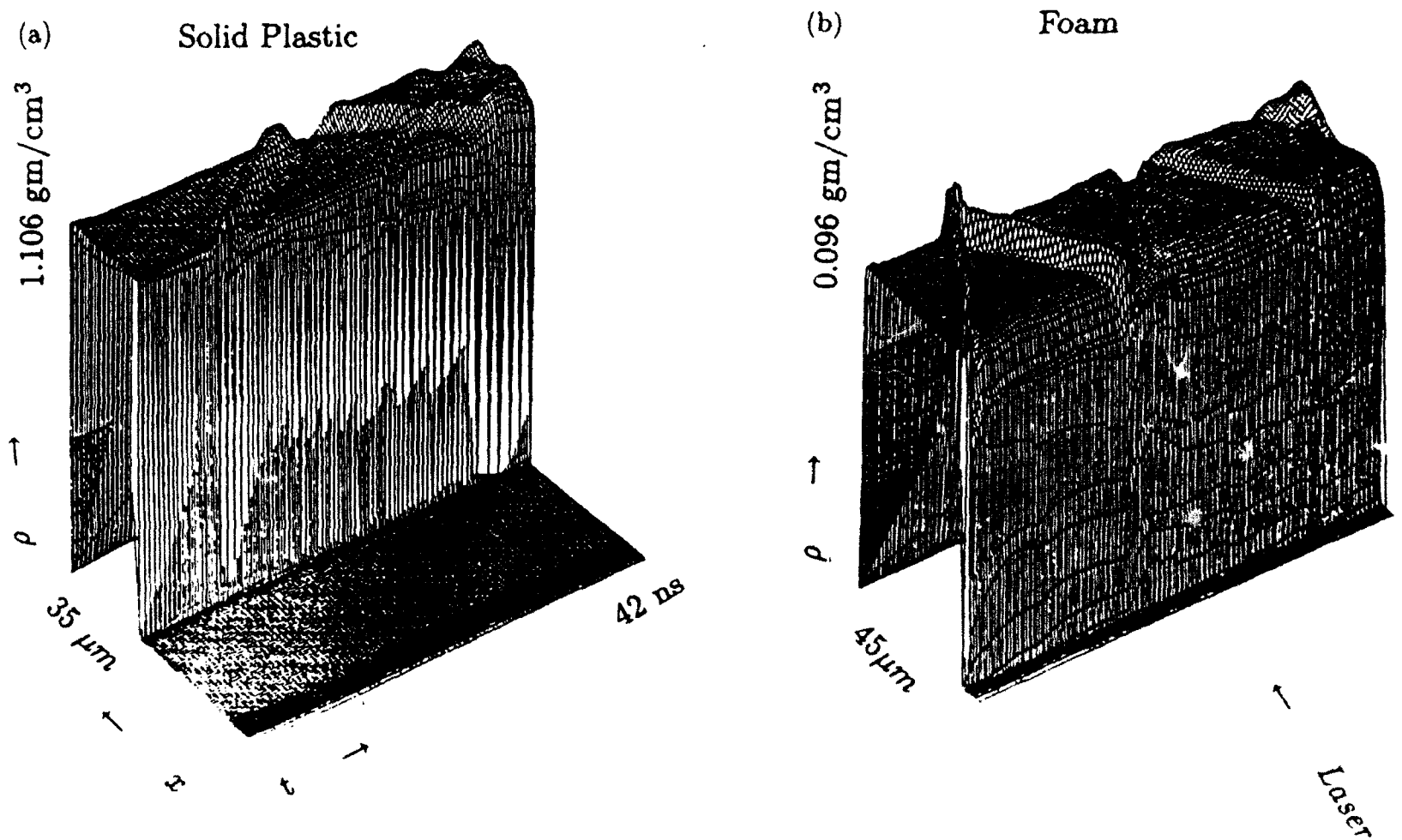

Figure 2. An x-t plot of the density illustrating the propagation characteristics of the elastic compression/tension waves through (a) the solid plastic and (b) the low density foam. The two materials are plotted separately for clarity.

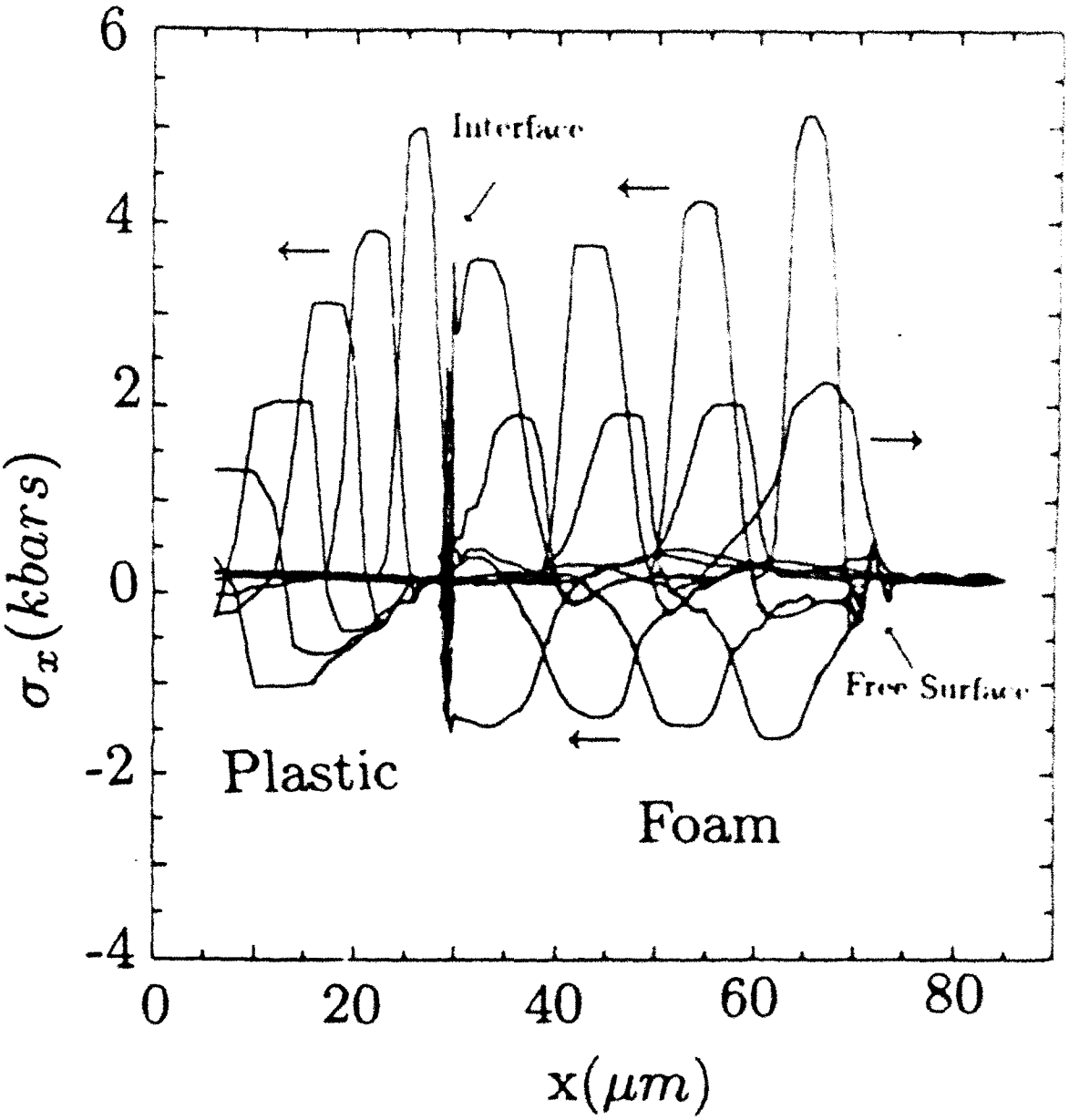

Figure 3. Plot of the amplitude of the elastic stress waves (σ_x (kilobars)) at 2 μsec intervals as the waves propagate through the foam-plastic target. The arrows indicate the direction of propagation.

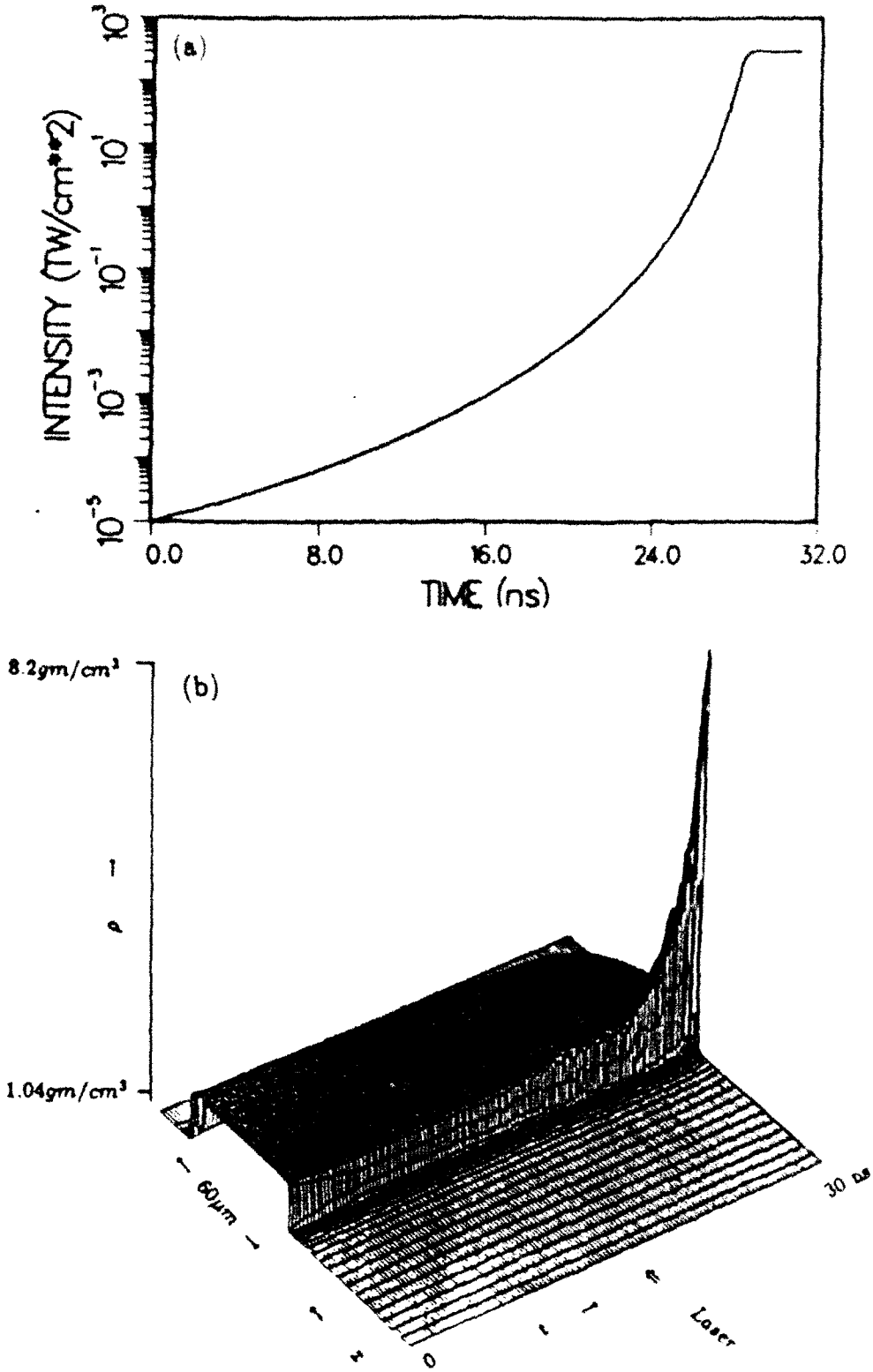

Figure 4. (a) Intensity profile for the temporally long, slowly rising laser pulse. (b) x-t-ρ plot for the 60 μm thick plastic target (in the center-of-mass frame) for the slowly rising laser pulse.

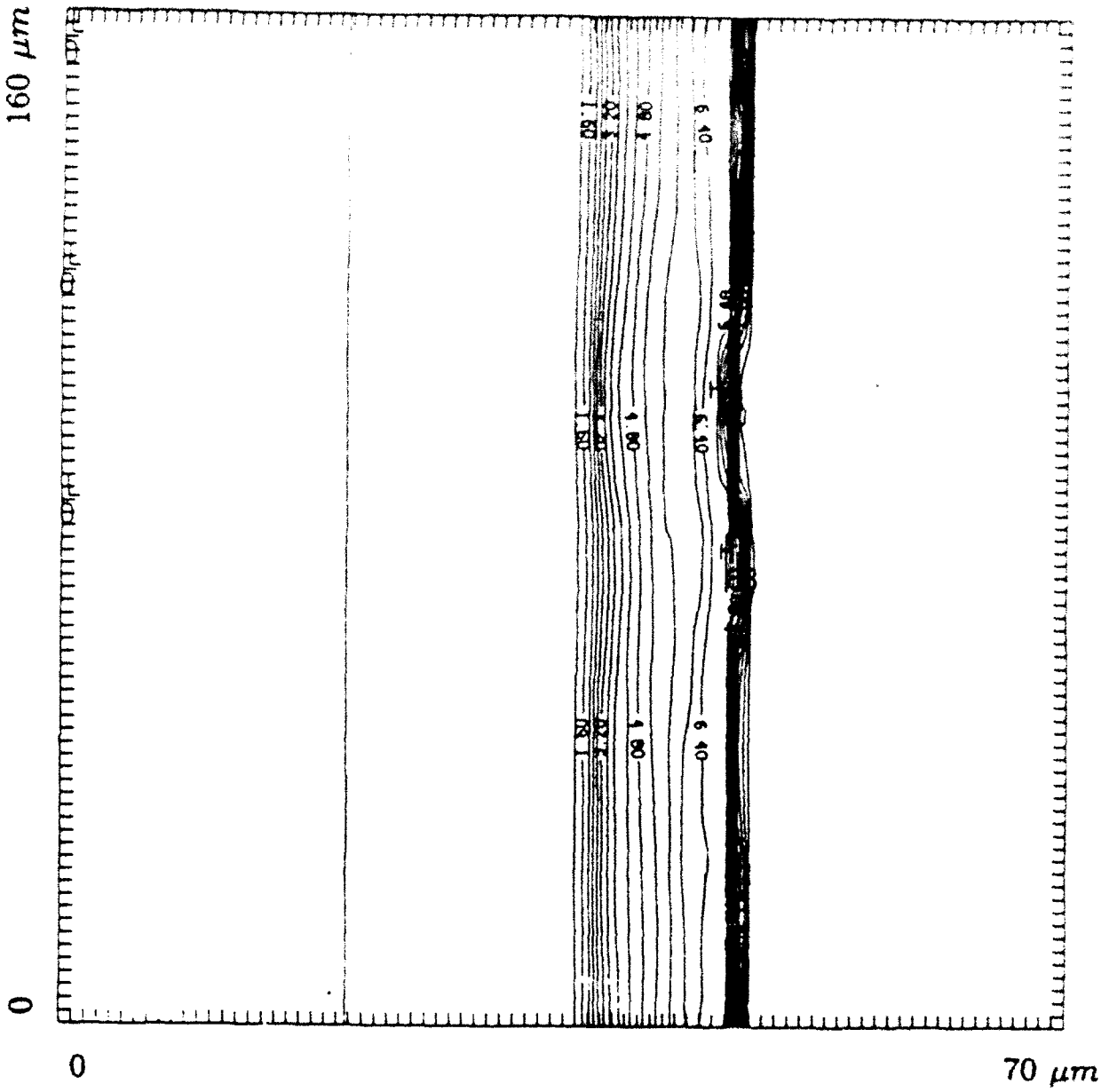

Figure 5. Isodensity contours of the 60 μm thick CH target at 28 nsec impacted with the slowly rising laser pulse. The maximum mass variation at this time is 0.5%.